Carbonates Evaporites (2016) 31:249–257
DOI 10.1007/s13146-015-0256-3

ORIGINAL ARTICLE

Origin of dedolomite in the Carboniferous of Eastern Sichuan basin and its geological significance

Wen Huaguo[1,2] · Cao Jixiang[2] · Wen Longbin[2] · Zheng Rongcai[1,2]

Accepted: 14 July 2015 / Published online: 15 August 2015

Abstract Resulting in dense lithology and poor physical properties, dedolomitization has detrimental effects on reservoir characteristics, so there has been little systematic research reported on the dedolomitization in the Carboniferous Huanglong Formation from the Eastern Sichuan basin. Through well drilling, well logging, thin-section authentication, and geochemistry tests, we studied for the first time the growth characteristics, regularities of distribution, genesis, and geological significance of dedolomitization in rock with typical fabric. From this study, we arrived at three conclusions: (1) the microstructure type divisions of dedolomite are as follows: A. a large micrite core and clear calcite rim, B. dolomite crystal, C. gypsum crystal, and D. rhombohedral pores; (2) rocks had low porosity and high density after dedolomitization in Eastern Sichuan, which is detrimental to reservoir development; and (3) micrite–microlite crystal dolomite and micrite–microlite crystal gypsum dolomite are the protoliths before dedolomitization. Sabkha is the primary sedimentary environment, in which the sabkha brine was kept within the layer and would become the main fluid of dolomitization in the high-quality dolomite reservoir from Eastern Sichuan. Analyzing the instances of dedolomitization has important geological significance in some ways, such as recovering the protolith, recovering the ancient environment, and discussing the relationships between diagenetic fluid properties and the reservoir's development.

Keywords Dedolomitization · Dedolomite · Origin · Paleokarst · Carboniferous · Eastern Sichuan basin

Introduction

Dedolomitization describes the process in which a gypsum evaporite is leached by meteoric water and underground water (rich in calcium and sulfur), resulting in the calcitization of early dolomite (Von Morlot 1847), and producing secondary limestone. Many scholars conducted experiments to study the mechanism (Katz 1968; Huang 2010; Choi et al. 2012) and found that dedolomitization could occur in both near-surface non-conformable contact environments (Boni et al. 2011; Vandeginste and John 2012) and shallow to deep diagenetic environments (Rameil 2008; Fu et al. 2008), but its influence on reservoir quality and the geological significance of the dedolomitization were still poorly understood (Choi et al. 2012; Wu et al. 2012; Zhang et al. 2012). The dolomite reservoir in the Carboniferous of the Eastern Sichuan basin is one of the most important reservoir types in China, about which there have been many studies (Hu et al. 2008; Zheng et al. 2008, 2010; Wen et al. 2009, 2011; 2014a, b). However, there has been no prior study of the origin or geological significance of the secondary limestone of the Huanglong 1st Formation in the Carboniferous. This article aims to reveal origin of the secondary limestone and further study the influence and geological significance to the reservoir by dedolomitization, through thin-section authentication and geochemical analysis.

✉ Wen Huaguo
wenhuaguo@qq.com

[1] State Key Laboratory of Oil and Gas Reservior Geology and Exploitation, CDUT, Chengdu 610059, China

[2] Institute of Sedimentary Geology, Chengdu University of Technology, Chengdu 610059, China

Regional geology

The total study area (Eastern Sichuan basin) is approximately 55,000 km^2, with Qi-Yue Mountain to the East, Huaying Mountain to the west, Daba Mountain to the North, and Chongqing-Kailong to the South. The Eastern Sichuan basin belongs to the Sichuan active tectonic zone, in which a large number of West-to-East steep structures exist (Fig. 1). In the Neopaleozoic period, the Eastern Sichuan basin was a gulf basin, which was surrounded by land and was located to the West of the craton basin on the East of the Yangtze plate. Then, in the early stage of the late Carboniferous epoch, the evaporites–carbonates of the Huanglong Formation overlapped with the dark shale of neritic shelf facies in the Silurian Hanjiadian Formation. In the middle-late stage of the late Carboniferous epoch, the Huanglong Formation experienced supergene karst for 15–20 Ma (Wen et al. 2009; Zheng et al. 1996) after Yunnan tectonic uplift and strong erosion in the Hercynian orogeny, so paleokarst features and systems developed near the top of this layer (Zheng et al. 2003) and resulted in one of the best paleokarst reservoirs. Then, the Huanglong Formation experienced two stages of tectonic deformation and fracturing: the Indosinian and Yanshanian orogenies, along with natural gas migration and accumulation, and formed a good-quality paleo-buried hill reservoir, which has huge potential for development and economic benefits.

The Huanglong Formation (C_2hl^1) is divided into three parts: (1) C_2hl^1, gypsum, crystallite dolomite, and secondary limestone; (2) C_2hl^2, grain dolomite, dolomite, mud dolomite, and microlite dolomite interbedding; and (3) C_2hl^3, microlite dolomite, grain microlite dolomite, and microlite-spar grain dolomite interbedding, with micrite–microlite dolomite in the interlayer. This paper aims to study the secondary limestone in the C_2hl^1.

Sedimentary characteristics

Types and structures

There are two main types of secondary limestone (secondary crystal limestone and secondary calcareous karst breccia), and each could also be divided into the following components: gypsum secondary limestone and dolomite secondary limestone.

Secondary crystal limestone (also called crystal limestone) is a type of limestone that is mainly formed by calcite (>50 %), with some dolomite fragments, quartz crystal pyroclasts, and small pores, and it often has massive structure and breccia structure.

Secondary calcareous karst breccia is a type of breccia that is usually formed by the collapse of a karst cave, with the breccia forming the secondary limestone. In the study area, the breccia is composed of secondary powder crystalline—

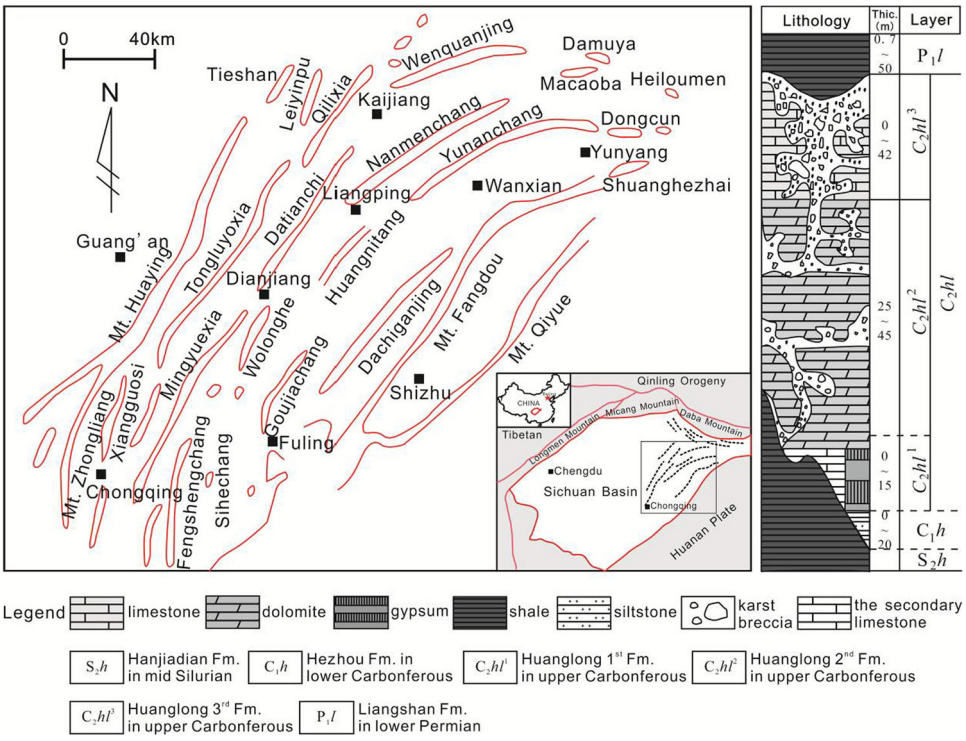

Fig. 1 Distribution layer of dedolomite and the tectonic construction of the Eastern Sichuan basin (modified from Wen et al. 2009)

fine crystalline limestone, the matrix of which is composed of secondary limestone fragments, calcites, quartz crystal pyroclasts, some enthetic dolomite fragments, and other materials. Secondary calcareous breccias can also be divided into three types for their contact relationships between breccias: (1) reticulate silt mosaic secondary calcareous karst breccia (Fig. 2b), (2) breccia-supporting secondary calcareous karst breccia (Fig. 2c), and (3) matrix-supporting secondary calcareous karst breccia (Fig. 2d), while the second type is the most common.

There are three types of structures of the secondary limestone: (1) dolomite pseudocrystal structure (rim structure), where micrite forms the core while clear calcite forms its rim; (2) dolomite pseudocrystal structure (dolomite crystal shape), where micrite grain aggregation forms a rhombus, or the grain calcite remains in the dolomite crystal; (3) gypsum pseudocrystal structure, where pykno mosaic calcite replaces the gypsum and remains in the gypsum crystal.

Dolomite pseudocrystal structure (rim structure)

The rhombus calcite aggregation formed the dolomite pseudocrystal structure, in which the micrite calcite remains in the core and its rim is lamella spar calcite (Fig. 2i). This clear calcite rim is regarded as formed by dedolomitization, in which the surrounded macro-crystal participates in the

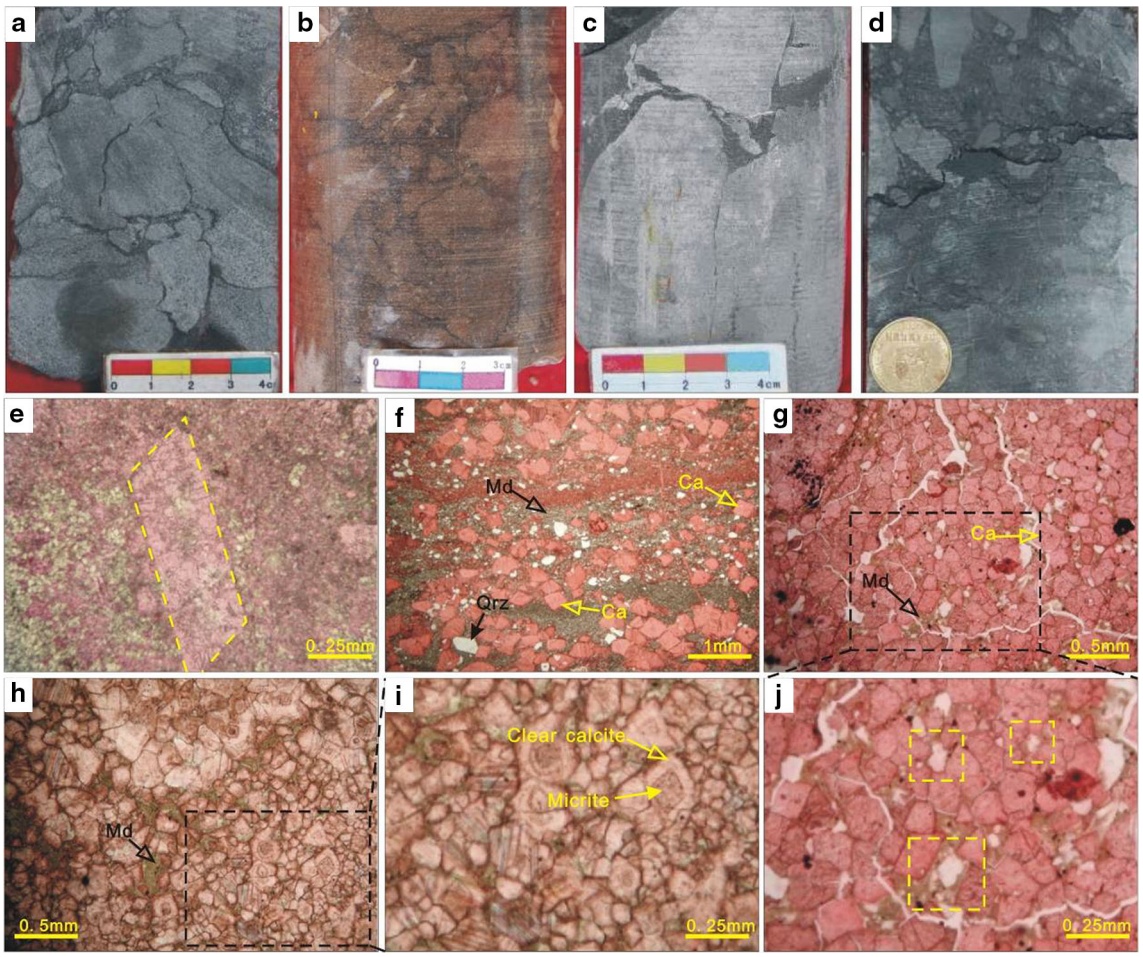

Fig. 2 Photographs showing the textures of dedolomite in the Carboniferous Huanglong 1st Formation, Eastern Sichuan basin. (Ca-calcite, Md-argillaceous components, Qz-quartz) **a**. Reticulate(Z1); **b**. reticulate silt mosaic secondary calcareous breccias(HL5); **c**. breccia-supporting secondary calcareous breccias, of which external peaty fillings occupy pores(MC1-1); **d**. matrix-supporting secondary calcareous breccias (BD12); **e**. dedolomite formed by dedolomitization and degypsification, while calcite (Ca) replaces gypsum and maintains the gypsum crystal form (TX1, PPL); **f**. laminated sand content argillaceous secondary limestone, of which secondary calcite maintains the dolomite crystal form, and quartz sands (Qrz) and argillaceous components (Md) are brought by ground water, exposing the karst process to dedolomite (W1, PPL); **g**. the secondary fine-grain limestones, of which secondary calcite (Ca) maintains the dolomite (Do) crystal form, and argillaceous components (Md) are brought by ground water and expose the karst process to dedolomite (W1, PPL); **h**. breccia-supporting secondary calcareous karst breccia, with a matrix formed by secondary calcite crystal pyroclasts and external argillaceous components (Md), where secondary calcite (Ca) has the dolomite (Do) appearance and girdle structure(T11, PPL); **i**. a large micrite core and clear calcite rim, in which the micrite and clear calcite replace, respectively, the core and the rim of dolomite crystals (PPL); and **j**. local amplification of the karst breccia dedolomite (PPL)

diagenetic process in the later stage, and remains in the dolomite crystal (Wen et al. 2014a). Some studies found that there is a mount of inclusions around the border between the core and the rim, so the rim more easily experiences dedolomitization (Wen et al. 2014b). The dedolomitization of dolomite usually happened from the border between the core and the rim. In the beginning, the dedolomitization grew into the core as micrite and then grew to the outside, forming the spar calcite around the core. Some scientists consider this rim structure as indicating the shallow buried digenetic environment (Gasparrini et al. 2006).

Dolomite pseudocrystal structure (dolomite crystal shape)

The calcite completely replaced the dolomite rhombus crystalline form and then formed the dolomite pseudocrystal structure (dolomite crystal shape). The secondary calcite in the Huanglong 1st Formation usually remains in the dolomite crystalline form, and with no straight boundary (Fig. 2f, g), the rhomb structure is clearly formed after the dedolomitization, with a single dolomite particle being replaced by calcite, which can be evidence for the dedolomitization. The dolomite pseudocrystal structure usually exists near the limestone mud (Fig. 2i), intraclasts (Fig. 2i), and the anaphase fillings (Fig. 2f). As one of the distinctive rock types in the Huanglong 1st Formation, the dolomite pseudocrystal structure (dolomite crystal shape) often has clear and recognizable borders, exists in the syngenetic micrite limestone, and is the most distinctive structure of the reburied carbonate fragments (Wen et al. 2014a).

Gypsum pseudocrystal structure

It had been confirmed that the dissolution of the gypsum is quite conducive to the dedolomitization process. The calcite was dissolved out in a way that preserved the gypsum shape, in which intensive micrite calcites remained (Fig. 2e). It is regarded that, with the leaching and corrosion of the atmospheric water to the gypsum, the concentrations of Ca^{2+} and SO_4^{2-} in liquid increased, and Mg^{2+} prefers to combine with SO_4^{2-} and moves with the liquid, and then CO_3^{2-} combined with Ca^{2+}, forming the calcite which slowly precipitated (Erik 2004), then developed the gypsum pseudocrystal structure. The solution, which is rich in SO_4^{2-}, more easily dissolves the dolomite crystal and develops dedolomitization.

Surface distribution

A thickness profile of the secondary limestone in the Huanglong 1st Formation (Fig. 3) was obtained, based on the statistics of the drilling data. Huanglong 1st Formation is 2–15 m in thickness, and some of the Western parts have thicker strata (Tieshan area and Xihekou area), while the central region (Liangping to West-North-Gou) has the thinnest strata of 0–2 m. Some erosion depressions (e.g., Shaguanping, Leiyinpu, and Zhangjiachang) have the largest thicknesses, while the thickness of the secondary limestone ranges from 2 to 10 m. The secondary limestone developed along the separation between regions of thin to thick layers (Fig. 3), where the high thickness area is from dill QL-3 to dill LB-3 and dill B-2 to dill W-102, and the low thicknesses are spread around Kaijiang–Liangping. At the same time, the thickness of the gypsum has almost the same tendency as the Huanglong 1st Formation (Fig. 3). Furthermore, the thicknesses of the gypsum and the secondary limestone have an inverse relationship (Fig. 3).

Study methods and results

All 30 samples for systematic testing and analysis were taken from drills in Huanglong 1st Formation far away from tectonics. For petrologic identification analysis under the microscope, all of the samples were collected using a micro-drill. The thin sections were identified using a microscope, and impurities and organic matter were eliminated. The procedures mentioned above were conducted to ensure the representativeness, accuracy, and reliability of the samples. The analyses of this study include thin-section observation, trace element analysis, and isotope analysis of carbon, oxygen, and strontium. The analytical data are shown in Table 1.

The double-polished casting thin sections (0.03 mm thick) were stained with Alizarin Red-S and potassium ferricyanide to distinguish calcite from dolomite and ferroan carbonate from non-ferroan carbonate.

The analyses of the trace elements (e.g., Fe, Mn, and Sr) were conducted at the Institute of Multipurpose Utilization of Mineral Resources, Chinese Academy of Geological Sciences, Chengdu, using a 2000 DV instrument, with a measured inaccuracy of 0.002 %. The analytic standard was Y/T05-1996 of the ICP broad-spectrum method.

The carbon–oxygen isotope test analysis was performed at the Research Institute of Exploration and Development, Southwest Oil and Gas Field Company, China National Petroleum Corporation, using a MAT252 gas isotope mass spectrometer. The analytic standard was SY/T 6039-94.

Sr isotope testing was performed at the State Key Laboratory of Oil and Gas Reservoir Geology and Exploitation using a MAT262 solid isotope mass spectrograph, and the measured inaccuracy (2σ) of $^{87}Sr/^{86}Sr$ is less than 0.002 %.

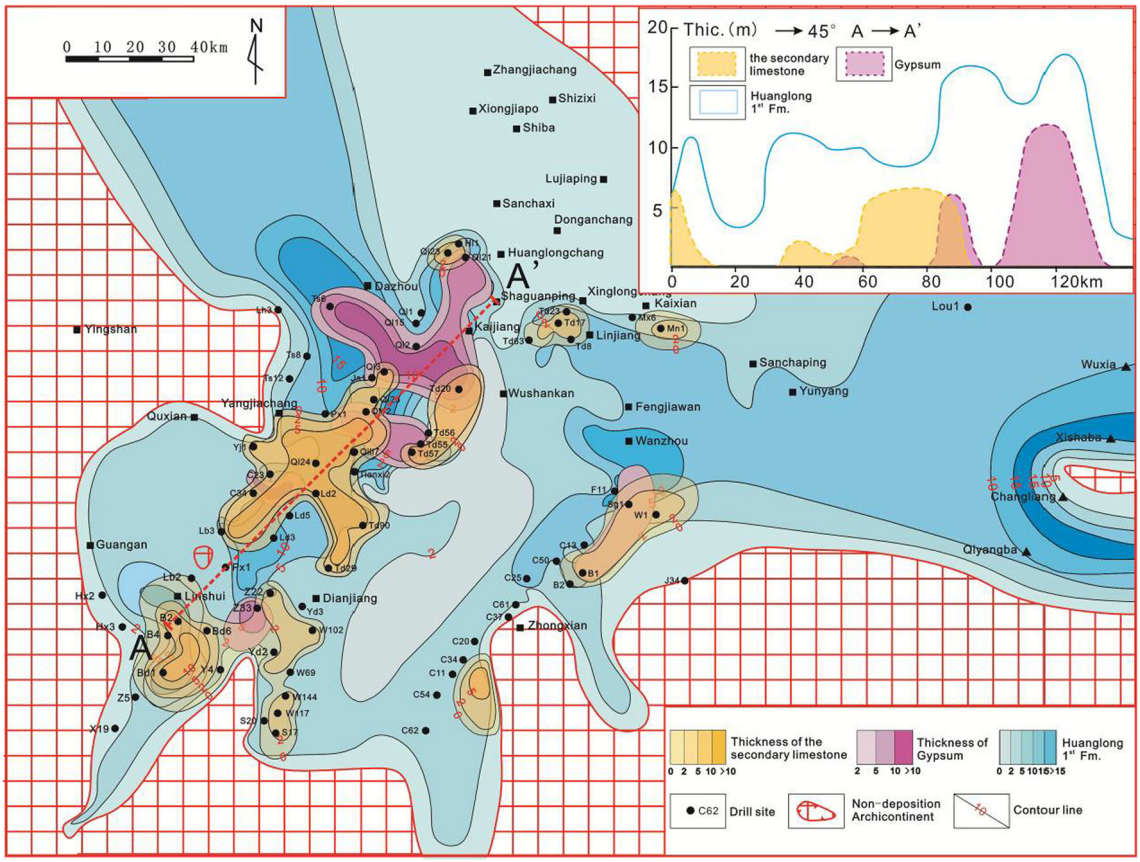

Fig. 3 Distribution of dedolomite and gypsum in the Carboniferous Huanglong 1st Formation, Eastern Sichuan basin

Discussion

Fe, Mn, and Sr

The characteristics of the scatter diagram for Fe, Mn, and Sr microelements are as follows:

1. The average concentrations in the secondary limestone are Fe 2082 ppm, Mn 173.2 ppm, and Sr 191.8 ppm, while the average concentrations in the secondary calcareous breccias are Fe 10,568 ppm, Mn 258 ppm, and Sr 211.8 ppm;
2. Fe in the secondary limestone is not as high and might be related to the matrix between the breccias or undissolved remnants near the ancient weathered crust (Huang 2010), or be related to the large distance to the unconformable surface (Wen et al. 2014b);
3. Sr in the secondary limestone is relatively abundant, and the secondary calcareous breccias have the highest concentrations. This might be because of two reasons: (1) the content of Sr in calcite ($CaCO_3$) is two times that of dolomite ($CaMgCO_3$) (Vahrenkamp and Swart 1990); and (2) the secondary calcareous breccias are a product of strong leaching.
4. Mn concentrations in the secondary limestone are high. The solution in the ancient karst process of the late Huanglong Formation leached the secondary limestone and left abundant Mn^{2+} in the matrix between the breccias, resulting in the secondary calcareous breccias having the highest Mn concentrations (Wu et al. 2012) (Fig. 4).

C and O isotopic geochemistry

1. The range of $\delta^{13}C$ in the secondary crystal limestone is −2.11 to 3.83 ‰ (−0.025 ‰ in average), while the secondary calcareous breccia is −2.92 to 3.73 ‰ (−0.49 ‰ in average); the range of $\delta^{18}O$ in the secondary crystal limestone is −8.929 to −5.12 ‰ (−7.03 ‰ in average), while the range in the secondary calcareous breccia is 5.96 to −2.90 ‰ (−3.958 ‰ in average) (Fig. 5).
2. The range of $\delta^{13}C$ and $\delta^{18}O$ in the secondary limestone is lower than those in the Moscovian marine carbonates (Table 1; Fig. 5), which may be related to one solution involved in the digenetic process with low ^{13}C and ^{18}O. Meteoric water has those characteristics (Veizer et al. 1999; Azmy et al. 2009).

Table 1 Characteristics of $\delta^{13}C$, $\delta^{18}O$, Sr^{87}/Sr^{86}, Fe, Mn, and Sr of dedolomite in the Carboniferous Huanglong 1st Formation, Eastern Sichuan basin

No	Sample no.	Lithology	$\delta^{13}C_{VPDB}$ (‰)	$\delta^{18}O_{VPDB}$ (‰)	$^{87}Sr/^{86}Sr \pm 2\sigma$	Fe (ppm)	Mn (ppm)	Sr (ppm)
1	BD13	Penecontemporaneous dolomite	2.31	−2.32	0.713622 ± 0.000056	810	89	105
2	HX16	Penecontemporaneous dolomite	2.67	−1.23	0.710290 ± 0.000058	980	112	374
3	J12	Penecontemporaneous dolomite	3.67	−1.22	0.718008 ± 0.000052	1400	100	108
4	QL35	Penecontemporaneous dolomite	2.57	−2.1	0.711753 ± 0.000096	830	66	102
5	T22	Penecontemporaneous dolomite	2.54	−3.04	0.713990 ± 0.000041	850	135	166
6	T24	Penecontemporaneous dolomite	2.89	−1.73	0.712877 ± 0.000041	760	105	140
7	YJ18	Penecontemporaneous dolomite	3.95	−1.47	0.709962 ± 0.000111	1600	92	95
8	YJ21	Penecontemporaneous dolomite	2.42	−1.23	0.709453 ± 0.000043	860	140	137
9	Z25	Penecontemporaneous dolomite	3.482	−1.869	0.713230 ± 0.000029	920	142	93
10	Z27	Penecontemporaneous dolomite	2.663	−2.124	0.715704 ± 0.000021	780	125	120
11	Z31	Penecontemporaneous dolomite	1.774	−1.14	0.711950 ± 0.000091	830	86	66
12	C61	The secondary crystal limestone	3.83	−8.47	0.712370 ± 0.000017	1200	180	209
13	W11	The secondary crystal limestone	−0.8	−6.87	0.716584 ± 0.000065	520	96	160
14	QL30	The secondary crystal limestone	−0.62	−6.37	0.709240 ± 0.000055	190	270	150
15	HL44	The secondary crystal limestone	−2.11	−6.43	0.711450 ± 0.000064	1600	200	240
16	BD34	The secondary crystal limestone	−1.532	−8.93	0.709640 ± 0.000054	1200	180	201
17	LD5	The secondary crystal limestone	1.08	−5.12	0.709031 ± 0.000062	6900	120	200
18	YJ17	The secondary calcareous breccias	−1.74	−4.08	0.709580 ± 0.000091	340	310	159
19	QL39	The secondary calcareous breccias	−2.92	−5.96	0.706789 ± 0.000104	1100	190	59
20	QL25	The secondary calcareous breccias	3.73	−2.90	0.715432 ± 0.000136	27600	140	291
21	MC1-1	The secondary calcareous breccias	1.12	−3.53	0.712340 ± 0.000081	5600	320	230
22	MC1-2	The secondary calcareous breccias	−2.66	−3.32	0.715369 ± 0.000074	18200	330	320

3. At the same time, the range of $\delta^{13}C$ and $\delta^{18}O$ in the secondary limestone is absolutely lower than the micritic-crystallite penecontemporaneous dolomite. This could be additional evidence for the meteoric water. With more meteoric water leaching, the $\delta^{18}O$ would be more negative (Gasparrini et al. 2006; Qian et al. 2013).

Sr isotope geochemistry

1. The $^{87}Sr/^{86}Sr$ ratios of the secondary crystal limestone range from 0.709031 to 0.716584 (0.711386 in average), while those of the secondary calcareous breccias range from 0.706789 to 0.715432 (0.711902 in average).
2. The $^{87}Sr/^{86}Sr$ ratios of the secondary crystal limestone are slightly higher than those of the Carboniferous Moscovian marine limestone (Veizer et al. 1999; Mcarthur et al. 2001) and are slightly lower than those of micritic-crystallite penecontemporaneous dolomite. There may be two reasons for this: (1) the leaching solution mixed with the interlayer solution, in which the dolomite formed and gathered ^{87}Sr, while the interlayer solution was depleted in ^{87}Sr. When the dedolomitization happened in the still undercurrent belt, the leaching solution would pass through and mix with the interlayer solution and result in a low ratio of $^{87}Sr/^{86}Sr$ in the leaching solution; and (2) the leaching solution inherited the low $^{87}Sr/^{86}Sr$ ratio of the original layer, and the solution in the still undercurrent belt maintains the low $^{87}Sr/^{86}Sr$ ratio of the original layer, so when the leaching solution arrived participated in the dedolomitization process, the dedolomite obtained the low $^{87}Sr/^{86}Sr$ ratio of the original layer (Fig. 6).

Origin and formation mode

The accepted chemical formula of the dedolomitization is as follows (aq, liquid; s, solid) (Zhang et al. 2012):

$$CaMg(CO_3)_2(s) + Ca^{2+}(aq) + SO_4^{2-}(aq) \Leftrightarrow 2CaCO_3(s) + Mg^{2+}(aq) + SO_4^{2-}(aq).$$

Recent experiments found that increasing concentrations of dissolved gypsum (in an appropriately wide range) in the buried environment will result in the decrease of Mg^{2+}/Ca^{2+}, Ca^{2+}/SO_4^{2-}, and Mg^{2+}/SO_4^{2-} ratios and finally approach 0.33, 0.79, and 0.26, respectively; so that additional gypsum dissolution occurs (in an appropriately wide

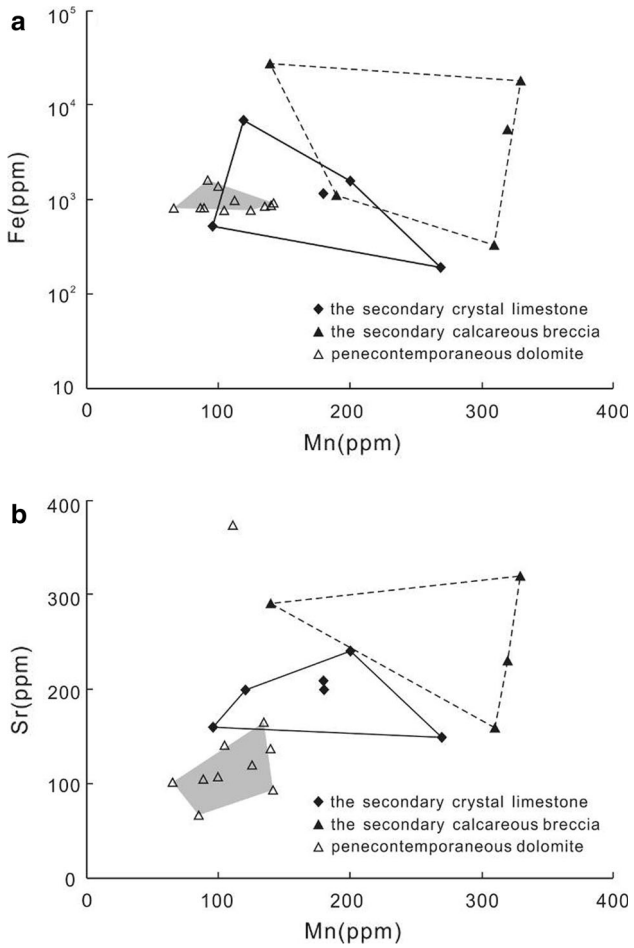

Fig. 4 Characteristics of Fe and Mn (**a**) and Sr and Mn (**b**) of dedolomite in the Carboniferous Huanglong 1st Formation, Eastern Sichuan basin

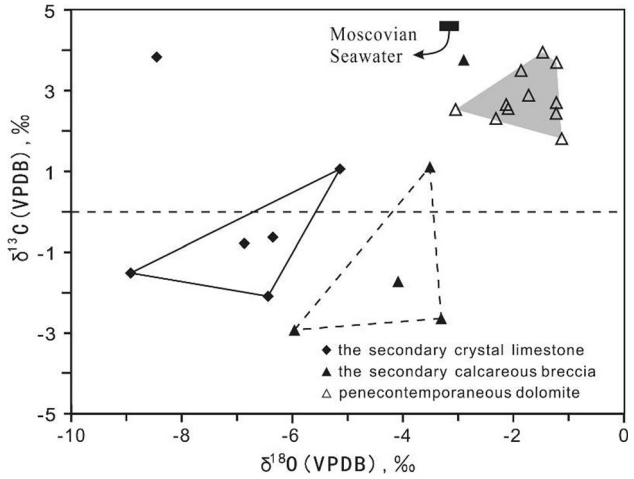

Fig. 5 Distribution of $\delta^{13}C$ and $\delta^{18}O$ of dedolomite in the Carboniferous Huanglong 1st Formation, Eastern Sichuan basin

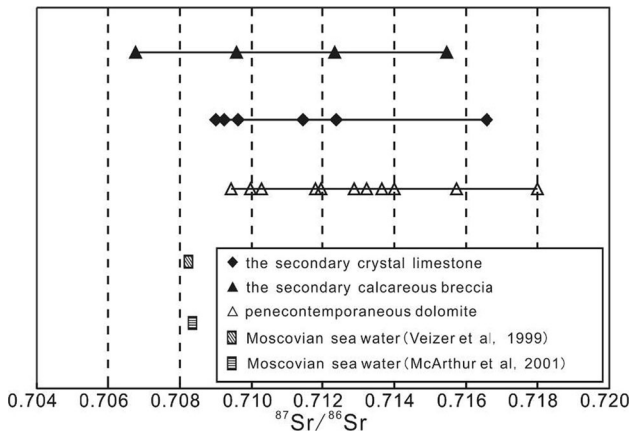

Fig. 6 Ratios of $^{87}Sr/^{86}Sr$ of the dolomite, secondary limestone of the Eastern Sichuan basin, and contemporary global marine limestone

range) and forms more secondary limestone (Choi et al. 2012). The chemical reaction is

$$0.32CaMg(CO_3)_2(s) + 1.32CaSO_4(s) \Leftrightarrow 0.64CaCO_3(s) + Ca^{2+}(aq) + 0.32Mg^{2+}(aq) + 1.32SO_4^{2-}(aq).$$

The formation process was that, in the middle to late stage of the late Carboniferous epoch, after the Yunnan tectonic uplift and strong erosion of the Hercynian orogeny, the Huanglong Formation experienced supergene karst for 15–20 Ma (Wen et al. 2009; Zheng et al. 1996) in the suddenly shallow buried digenetic environments which developed holes and gaps to supply effective channels for meteoric water and interlayer water. The resulting layer sequence is composed of marine limestone–dolomite–gypsum–mud from top to bottom. Water will flow through and leach the gypsum layer and become a gypsum solution.

This gypsum solution is a solution with high SO_4^{2-} levels and a high Ca/Mg ratio. It kept leaching the break in the intergranular seam of the dolomite below, in which Ca^{2+} in the solution would replace Mg^{2+} in the dolomite and form the secondary limestone until the ratio of Ca/Mg reached a high enough value (Erik 2004). In the relatively shallow buried environment, with relatively low pressure and temperature, the solution that leached the gypsum would be of lower pH, could accelerate the dissolution of the dolomite, and would create more space for the precipitation of secondary limestone (Huang 2010). Then, the degypsification would result in the layer collapse and form the secondary calcareous breccias (Zhao et al. 2012).

The dedolomitization happened in the still undercurrent belt, in which the solution moved slowly and quick crystallization and materials such as mud–limestone, dolomite fragments, and mud residuals filled voids in the calcite breccias and the crystal limestones, which was detrimental to the reservoir quality (Fig. 7). Additionally, the calcite is

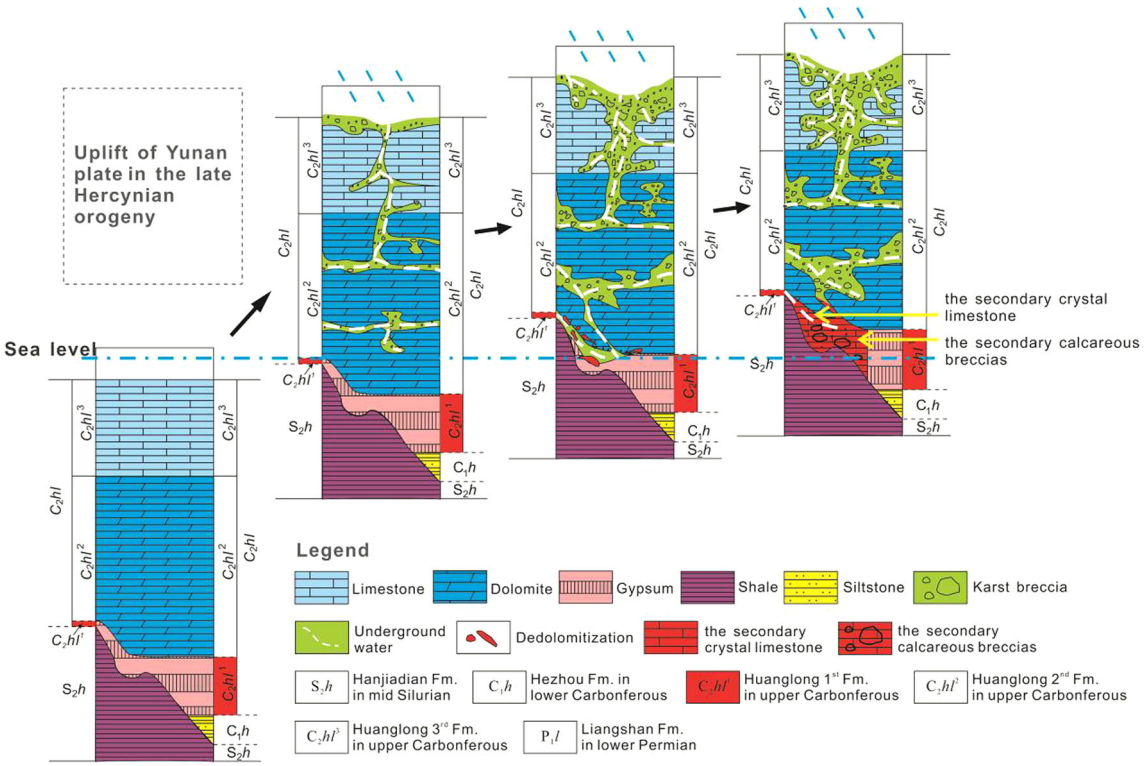

Fig. 7 Genesis of dedolomite in the Carboniferous Huanglong 1st Formation, Eastern Sichuan basin

larger than the dolomite in crystal form (Huang 2010), which was also detrimental to the reservoir quality.

Conclusion

1. The secondary limestone in the study area mainly includes secondary crystal limestone, secondary calcareous breccias, and some gypsum dolomite secondary limestone. Due to relatively larger crystal size of Ca_2CO_3 to $CaMgCO_3$, and unstable holes in it after dedolomitization, the secondary limestone has little holes. Among the secondary calcareous breccias, the mud limestone, dolomite fragments, mud residuals, and calcite cements became trapped in the pores of the still undercurrent belt. Therefore, both the secondary crystal limestone and the secondary calcareous breccias in the study area have high density and small pores, which would not form a reservoir without additional leaching.
2. Based on the slice analysis, the recognized remnant dolomite crystal and gypsum crystal from the secondary calcite were replaced by dedolomitization and degypsumization; so the original rock is micrite-crystallite dolomite and gypsum micrite-crystallite dolomite. Based on the rock and the regional geology, the original environment of the Huanglong 1st Formation was sabkha. The original dolomite in the Huanglong 1st Formation was micrite-crystallite dolomite, and gypsum micrite-crystallite dolomite formed in the penecontemporaneous stage, in hot weather, with the evaporation pump function (Hu et al. 2008). The study of the origin of the secondary limestone would help recover the ancient sedimentary and hydrological environment and provide evidence for the lithofacies paleogeography of the Huanglong Formation in the eastern Sichuan basin.
3. It has been confirmed that (Zheng et al. 2010; Wen et al. 2011) the dolomitization solution for the grain dolomite and dolomite breccias, which constitute the best reservoir of Huanglong 2nd Formation, is the sabkha brine trapped in Huanglong 1st Formation (Wen et al. 2014a). This article also supported the conclusion that the formation environment of the secondary limestone in Huanglong 1st Formation is sabkha and provided a way to study the nature of the diagenetic solution.

Acknowledgments This work was supported by the National Natural Science Foundation of China (Grant No. 41002033), National Major Science and Technology specific project of China (2011ZX05030—003—02), Natural Science key project of Education Department in Sichuan (13ZA0058), and the Foundation for Fostering Middle-aged and Young Key Teachers of Chengdu University of Technology.

References

Azmy K, Knight I, Lavoie DCG (2009) Origin of dolomites in the boat harbour formation, St. George Group, in Western Newfoundland, Canada: implications for porosity development. Bull Can Pet Geol 57(1):81–104

Boni M, Mondillo N, Balassone G (2011) Zincian dolomite: a peculiar dedolomitization case? Geology 39:183–186

Choi BY, Yun ST, Mayer B (2012) Hydrogeochemical processes in clastic sedimentary rocks, South Korea: a natural analogue study of the role of dedolomitization in geologic carbon storage. Chem Geol 306–307:103–113

Erik F (2004) Microfacies of carbonate rocks-analysis, interpretation and application. Springer, Berlin, pp 325–334

Fu QL, Qing HR, Bergman KM et al (2008) Dedolomitization and calcite cementation in the middle Devonian Winnipegosis formation in central Saskatchewan, Canada. Sedimentology 55:1623–1642

Gasparrini M, Bechstaedt T, Boni M (2006) Massive hydrothermal dolomites in the Southwestern Cantabrian Zone (Spain) and their relation to the late Variscan evolution. Mar Pet Geol 23(5):543–568

Hu ZG, Zheng RC, Wen HG et al (2008) Dolostone genesis of Huanglong Formation of Carboniferous in Linshui of Eastern Sichuan-Northern Chong qing area. Acta Petrol Sin 24(6):1369–1378

Huang SJ (2010) Diagenesis of carbonatite. Geological Publishing House, Beijing

Katz A (1968) Calcian dolomites and dedolomitization. Nature 217:439–440

Mcarthur JM, Howarth RJ, Bailey TR (2001) Strontium isotope stratigraphy: lowess version 3: best fit to the marine Sr-Isotope curve for 0–509 Ma and accompanying look-up table for deriving numerical age. J Geol 109:155–170

Qian YX, Sha XG, Li HL et al (2013) An approach to caledonian unconformities and sequence stratigraphic patterns and distribution of reservoirs of ordovician carbonate in the Western Tazhong area, Tarim basin. Earth Sci Front 20(1):260–274

Rameil N (2008) Early diagenetic dolomitization and dedolomitization of late jurassic and earliest cretaceous platform carbonates: a case study from the Jura Mountains(NW Switzerland, E France). Sed Geol 212:70–85

Vahrenkamp VC, Swart PK (1990) New distribution coefficient for the incorporation of strontium into dolomite and its implications for the formation of ancient dolomites. Geology 18:387–391

Vandeginste V, John CM (2012) Influence of climate and dolomite composition on dedolomitization: insights from a multi-proxy study in the Central Oman mountains. J Sediment Res 82:177–195

Veizer J, Ala D, Azmy K et al (1999) $^{87}Sr/^{86}Sr$ ^{13}C and ^{18}O evolution of Phanerozoic sea water. Chem Geol 161(1–3):58–88

Von Morlot A (1847) über Dolomit und seine künstliche Darstellung aus Kalkstein[C]. In: Von Haidinger W (ed) Naturwissenschaftliche Abhandlungen: Gesammelt und durch Subscription lursg, 1:305–315

Wen HG, Zheng RC, Shen ZM et al (2009) Study on the Carboniferous Palaeokarst landform in Eastern Sichuan basin. Geol Rev 55(6):816–827

Wen HG, Zheng RC, Shen ZM et al (2011) Sedimentary-diagenetic systems of Carbonatite reservoirs in the Huanglong formation, Eastern Sichuan Basin. Earth Sci J Chian Univ Geosci 36(1):111–121

Wen HG, Chen HR, Wen LB et al (2014a) Diagenetic fluids of paleokarst reservoirs in Carboniferous from Eastern Sichuan basin: some evidences from fluid inclusion, trace element and C, O, Sr isotope. Acta Petrol Sin 30(3):655–666

Wen HG, Wen LB, Chen HR et al (2014b) Geochemical characteristics and diagenetic fluids of dolomite reservoirs in the Huanglong formation, Eastern Sichuan Basin, China. Pet Sci 11(1):52–66

Wu SQ, Qian YX, Li HL et al (2012) Characteristics and main controlling factors of dolostone reservoir of the middle–lower Ordovician Yingshan formation in Katak uplift of Tarim basin. J Palaeogeogr 14(2):209–218

Zhang J, Shou JF, Wen YC et al (2012) Mechanism of dedolomitization and its rebuilding to reservoir. J Palaeogeogr 14(1):69–84

Zhao WZ, Shen AJ, Hu SY (2012) Types and distributional features of Cambrian–Ordovician dolostone reservoirs in Tarim basin, Northwestern China. Acta Petrol Sin 28(3):758–768

Zheng RC, Zhang SN, Li DM (1996) Origin of the karstic breccias in the Eastern Sichuan basin, and its significance. J Chengdu Univ Technol 23(1):8–18

Zheng RC, Peng J, Gao HC (2003) Palaeokarst-related characteristics of carbonate reservoirs in Huanglong Formation, upper Carboniferous, Eastern Chongqing. Geol-Geochem 31(1):28–35

Zheng RC, Hu ZG, Zheng C et al (2008) Geochemical characteristics of stable isotopes in paleokarst reservoirs in Huanglong formation in Northern Chongqing eastern Sichuan area. Earth Sci Front 15(6):303–311

Zheng RC, Dang LR, Zheng C et al (2010) Diagenetic system of carbonate reservoir in Huanglong Formation from East Sichuan to North Chongqing area. Acta Petrol Sin 31(2):237–249